

Self- and Interdiffusion in Ternary Cu–Fe–Ni Alloys

S.V. Divinski^{1, a}, F. Hisker¹, Chr. Herzig¹,
R. Filipek^{2, b}, M. Danielewski²

¹ Institute for Materials Physics, University of Münster,
Münster, Germany

² AGH University of Science and Technology, al.Mickiewicza 30,
30-059 Krakow, Poland

^a divin@uni-muenster.de, ^b rof@agh.edu.pl

Keywords: Cu-Fe-Ni, tracer diffusion, interdiffusion, ternary alloy, radiotracer measurement, Darken method, Danielewski-Holly model

Abstract. Diffusion of ⁶⁴Cu, ⁵⁹Fe, and ⁶³Ni radiotracers has been measured in Cu–Fe–Ni alloys of different compositions at 1271 K. The measured penetration profiles reveal grain boundary-induced part along with the volume diffusion one. Correction on grain boundary diffusion was taken into account when determining the volume diffusivities of the components. When the Cu content in the alloys increases, the diffusivities increase by order of magnitude. This behaviour correlates well with decreasing of the melting temperature of corresponding alloys, as the Cu content increases.

Modelling of interdiffusion in the Cu–Fe–Ni system based on Danielewski-Holly model of interdiffusion is presented. In this model (extended Darken method for multi-component systems) a postulate that the total mass flow is a sum of the diffusion and the drift flows was applied for the description of interdiffusion in the closed system. Nernst-Planck's flux formula assuming a chemical potential gradient as a driving force for the mass transport was used for computing the diffusion flux in non-ideal multi-component systems.

In computations of the diffusion profiles the measured tracer diffusion coefficients of Cu, Fe and Ni as well as the literature data on thermodynamic activities for the Cu–Fe–Ni system were used. The calculated interdiffusion concentration profiles (diffusion paths) reveal satisfactory agreement with the experimental results.

Introduction

Advanced materials are very often multi-component and have complex structure (gradient materials, coatings, etc.) and from thermodynamic point of view are non-ideal. Interdiffusion and interfacial reactions play important role during processing of many functional materials and limit their long term exploitation. Understanding of these processes has fundamental practical importance.

There are different approaches to reach this goal. These are Onsager phenomenology [1] and Darken method [2], they differ in form of the constitutive flux formula. Up to now they were not unified and the fundamental question is whether the computed diffusivities or interdiffusion coefficients represent real material constants [3]. Situation is even more difficult because the proof of the uniqueness of the inverse Darken problem does not exist [4].

We selected relatively simple Cu-Fe-Ni system to study the interdiffusion in non-ideal alloys showing limited solubility. This system has advantage because its thermodynamic and kinetic data are fairly well known. This paper has two goals: first to measure the tracer diffusivities of all components as a function of the ternary alloy composition, second the theoretical examination of the extended Darken method (Danielewski-Holly model) for a ternary system.

Experimental measurements

Sample preparation and radiotracer measurements

Copper, iron and nickel (99.99 pct purity) were used as starting materials. The ternary alloys (Table 1) were melted in induction furnace in argon atmosphere. Such obtained ingots were homogenized at 1273 K for 250 hour in argon ($p_{O_2} < 10^{-6} atm$). Subsequently, the alloys of different composition were reannealed at the temperature 50 °C below their melting temperature for 4 hours for recrystallization. The grain size of polycrystalline alloys was measured to vary from 30 (Cu-richest alloy) to about 300 μm .

Alloys in the form of the cylindrical ingots of 8 mm in diameter were cut into slices of 3 mm thick by spark erosion. One face of the specimen was polished to optical quality by standard metallographical procedure. The samples were encapsulated into Cu–Fe–Ni containers (made of nearly the same alloy which was under study), wrapped in Ta foil, and sealed in silica tubes under purified Ar atmosphere. The use of the containers guarantees that the chemical composition of the specimen was not changed during thermal treatment. The samples were subsequently annealed at 1373 K for 24 h in order to remove the mechanical stresses, which could be built up during cutting and polishing procedures and which could affect the diffusion behaviour. After the pre-annealing the blank surface was slightly chemically polished with Syton colloidal silica slurry to remove the effects of thermal etching.

Table 1. Alloy compositions in wt. %

Alloy	Fe	Ni	Cu
#1	12	68	20
#2	25	50	25
#3	10	45	45
#4	28	37	35
#5	45	40	15
#6	6	24	70
#7	75	20	5
#8	10	80	10

Penetration profile measurements

The radiotracer ^{64}Cu (half-life 12.7 hours) was produced by neutron irradiation of a copper chip at the research reactor in Geesthacht, Germany. The nuclear reaction $^{63}_{29}Cu(n,\gamma)^{64}_{29}Cu$ was used. Its initial specific activity was about 500 MBq/mg. Due to short life-time of the isotope it was delivered to the lab in Münster in few hours after irradiation. The activated chip was dissolved in nitric acid and then diluted with double-distilled water.

The radiotracer ^{59}Fe (half-life 45 days) was also produced by neutron irradiation of iron powder at the research reactor in Geesthacht according to the nuclear reaction $^{58}_{26}Fe(n,\gamma)^{59}_{26}Fe$. The activated isotope material was dissolved in 30% HCl and then further diluted with double-distilled water.

The radiotracer ^{63}Ni (half-life 100 years) was purchased in form of a HCl solution and dissolved with double-distilled water.

Each radiotracer (^{64}Cu , ^{59}Fe , or ^{63}Ni) was dropped as a dilute acid solution on the polished face of the samples. The samples were again encapsulated into containers, which were then wrapped into Ta foil, to avoid any undesirable contamination. The specimens were sealed in silica tubes under

purified Ar atmosphere and subjected to the diffusion anneals at $T = 1271$ K. The temperatures were measured and controlled with Ni–NiCr thermocouples with an accuracy of about ± 1 K. After the diffusion anneal the samples were reduced in diameter (at least 1 to 2 mm) by grinding on a lathe to remove the effect of lateral and surface diffusion.

The penetration profiles were determined by the precision grinding sectioning technique using special abrasive mylar foils. The radioactivity of each section was determined with high efficiency using a Packard TRI CARB 2500 TR liquid scintillation counter.

The penetration profiles present the plots of the normalized activity of each sections (the activity divided by the weight of the section) against the penetration depth x . The latter was calculated from the weight loss of the sample with known geometry after each sectioning step.

The uncertainties of individual points on the penetration profiles, stemming from the counting procedure and the errors of the depth determination, were estimated to be typically less than 10 %.

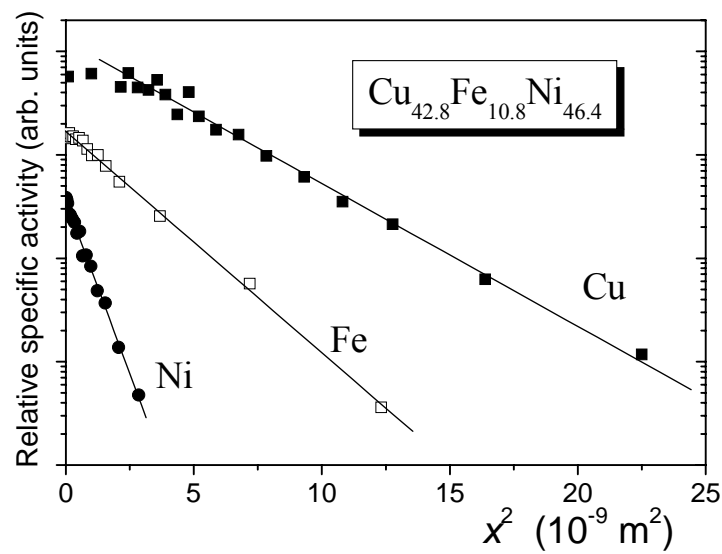


Figure 1. Penetration profiles for ^{63}Ni (circles), ^{59}Fe (open squares), and ^{64}Cu (filled squares) radiotracer diffusion in the alloy #3 measured at $T = 1271$ K, x is the penetration depth.

Results

Radiotracer experiments

All penetration profiles measured in the present work (especially in the case of Fe diffusion) show grain boundary and volume diffusion parts. Since we are mainly interested in volume diffusivities in the present study, the grain boundary contribution has to be carefully subtracted. We performed numerical fitting of the profiles accounting for both, volume and grain boundary diffusion.

The deepest part of the penetration profiles, which represents the grain boundary diffusion contribution, should be linear in the coordinates of $\ln \bar{c}$ vs. $x^{6/5}$ according to general Suzuoka's solution [5]. Here \bar{c} is the radiotracer concentration (specific activity) in a layer perpendicular to the penetration depth x . These conditions are indeed realized in our experiments, which correspond to Harrison's B-type [6] grain boundary diffusion regime. Then, the product $P = s \cdot \delta \cdot D_{\text{gb}}$ of the pertinent segregation factor s , the grain boundary width δ , and the grain boundary diffusivity D_{gb}

can be determined from the corresponding slope of the deepest part of the penetration profiles as given by [5]:

$$P = 1.084 (D^*)^{0.469} t^{0.531} \left(\frac{\partial \ln \bar{c}}{\partial x^{6/5}} \right)^{-1.718} \quad (1)$$

where D^* and t are the volume diffusion coefficient and the diffusion time, respectively. Accounting for the exact solution of the grain boundary diffusion problem, Eq. (1), the grain boundary diffusion contribution can correctly be subtracted from the measured experimental profiles.

Resulting penetration profiles measured for ^{63}Ni , ^{59}Fe , and ^{63}Cu diffusion in Cu–Fe–Ni alloys follow the Gaussian solution of the diffusion problem ($\ln \bar{c}$ vs. x^2). In total 24 penetration profiles were measured. As an example, in the Figure 1 the penetration profiles (corrected, after subtracting the grain boundary diffusion contribution) measured in the alloy #3 are presented.

The volume tracer diffusivity D^* can then be determined from the slope of the penetration profiles in the coordinates $\ln \bar{c}$ vs. x^2 :

$$D^* = \frac{1}{4t} \left(\frac{\partial \ln \bar{c}}{\partial x^2} \right)^{-1} \quad (2)$$

In the Figure 2 the Ni tracer diffusion coefficient D^*_{Ni} is plotted as a function of the alloy composition at $T = 1271$ K using iso-diffusivity lines. In order to draw this diagram it was assumed that the logarithm of the Ni diffusivity varies linearly between the measured compositions.

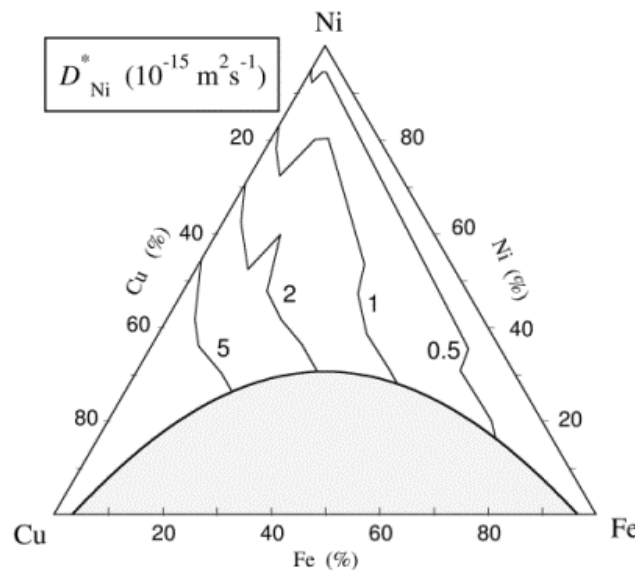


Figure 2. Ni tracer diffusivity measured in Cu–Fe–Ni alloys at 1271 K as a function of the composition (wt. %). The lines are drawn for a constant diffusivity which is indicated in $10^{-15} \text{ m}^2/\text{s}$ units. The two-phase region is marked by light-grey.

Generally, Ni diffuses most slowly in the Cu–Fe–Ni alloys with respect to the other tracers and Cu is the fastest component. The difference in the component diffusivities varies by factor 3 (in the alloy #8) to more than order of magnitude (in the alloy #3).

When Cu content in the alloys increases, the diffusivities also increase. This behaviour correlates with successive lowering of the melting temperature of corresponding alloys, as the Cu content increases. Since the measurements were performed at 1271 K, the normalized temperature

(relatively to the melting temperature of the alloy) varies from about 0.7 for Ni and/or Fe rich samples to about 0.9 for the Cu-richest specimen.

Modelling of Interdiffusion in the Cu-Fe-Ni Alloys and its Experimental Verification

Using the tracer diffusivities of Cu, Fe, and Ni as well as the thermodynamic activity data, the modelling of interdiffusion in Cu-Fe-Ni alloys was performed using Danielewski-Holy model of interdiffusion [7,8]. In this section mathematical model of interdiffusion as well as thermodynamic and kinetic data for the Cu-Fe-Ni system are analyzed. Finally, the computed concentration profiles are compared with the experimental results.

Model

The Danielewski-Holy model of interdiffusion for multi-component systems allows quantitative description of the complex diffusion mass-transport process for the unlimited number of elements and when the tracer diffusion coefficients are concentration dependent. It allows calculation of time evolution of the components' concentration profiles for non-ideal systems when thermodynamic activity data are available. The details of this model can be found elsewhere [7,8]. A short formulation of the initial-boundary-value problem for the interdiffusion in a closed system necessary for understanding the rest of the paper is presented here.

Data: 1) The self (tracer) diffusivities[†] of the components: D_1^*, \dots, D_r^* , where $D_i^* = D_i^*(N_1, \dots, N_r)$, 2) the thermodynamic activities of the components: $a_i = a_i(N_1, \dots, N_r)$, where N_i is the mole fraction of i -th component, 3) the time of the process duration: \hat{t} and 4) the thickness of the system: 2Λ .

Physical laws: 1) the law of the mass conservation of an i -th component:

$$\frac{\partial c_i}{\partial t} = -\frac{\partial J_i}{\partial x} \quad (i = 1, \dots, r). \quad (3)$$

Following Darken drift flow idea we postulate that the flux of an i -th element is a sum of the diffusion flux, J_i^d , and drift flux:

$$J_i = J_i^d + c_i v \quad (4)$$

The effective solution of this model was obtained using Nernst-Panck diffusion flux formula [10]:

$$J_i^d = B_i c_i \sum_j F_j, \quad (5)$$

where B_i is the mobility of an i -th component and $\sum_j F_j$ - the sum of the local driving forces, e.g., chemical potential gradient and/or the electrical field (for charged species), the gravitational force (in the sedimentation experiments) [11].

2) *Postulate of the constant mixture concentration*, i.e., the equation of state, which tells that the sum of concentrations of all elements at any position and for every time is constant:

[†] Correlation effects in multi-component alloys are often neglected and vacancy-wind factor doesn't differ much from unity [9]. Moreover one has to accept the fact that the experimental error(s) are the same order of magnitude or exceed expected effect. Thus, one can assume that self- and tracer diffusion coefficients are equivalent in multi-component alloys.

$$c_1 + \dots + c_r = c = \text{const.} \quad (6)$$

Initial and boundary conditions: 1) the initial concentration profiles of the components in the system $c_i(0, x) = c_i^o(x)$, where $x \in [-\Lambda, \Lambda]$ 2) the fluxes of the components through the boundary: $J_i(t, \pm\Lambda) = 0$, i.e., the system is closed.

Unknowns: 1) the concentration profiles of all elements as a function of time $c_i(t, x)$ and 2) the drift velocity $v_i(t, x)$.

The Diffusion Flux Formula

Equation (5) describing the diffusion flux can be rearranged into the form, which has been used in the numerical solution. It is generally accepted, that in metallic systems (alloys) the diffusion force in Eq. (5) can be described as the spatial gradient of the chemical potential, μ_i , and the corresponding flux can be expressed by the following expression

$$J_i^d = -B_i c_i \frac{\partial \mu_i}{\partial x}. \quad (7)$$

The chemical potential is defined by

$$\mu_i(c_1, \dots, c_r) = \mu_i^o + kT \ln a_i(c_1, \dots, c_r), \quad (8)$$

where k – the Boltzmann's constant, T – an absolute temperature and μ_i^o is the standard-state chemical potential usually referred to unit thermodynamic activity ($a_i = 1$). The gradient of the chemical potential can be calculated as follows

$$\frac{\partial \mu_i}{\partial x} = \sum_{j=1}^r \frac{\partial \mu_i}{\partial c_j} \frac{\partial c_j}{\partial x}. \quad (9)$$

Using Eqs. (7), (8), (9) and substituting the Nernst-Einstein relation ($D_i^* = B_i kT$) the diffusion flux can be expressed as follows:

$$J_i^d = -D_i^* c_i \sum_{j=1}^r \frac{\partial \ln a_i}{\partial c_j} \frac{\partial c_j}{\partial x}. \quad (10)$$

Above diffusion flux formula can be rearranged to

$$J_i^d = -\sum_{j=1}^r D_{ij} \frac{\partial c_j}{\partial x}, \quad (11)$$

where the partial intrinsic diffusivities, D_{ij} , are defined as follows

$$D_{ij} := D_i^* c_i \frac{\partial \ln a_i}{\partial c_j}. \quad (12)$$

Solution of the Model

The solution of the presented model was obtained in several steps:

(1) mathematical reformulation of the problem, (2) formulation of the generalized solution, (3) numerical solution using Galerkin-like method, which reduce an infinite dimension problem to finite one, (4) solving the resulting system of ordinary differential equations, (5) computer implementation of method – DIFSIM software [12]. The details on the solution can be found elsewhere [8,13].

Approximation of Thermodynamic Data for Cu-Fe-Ni Alloys

Cu-Fe-Ni system at 1273 K has a miscibility gap and a wide single phase region (Fig. 3). Thermodynamic data for this system has been assessed by Jansson [14] and re-evaluated by Rönka et al [15]. In the Figure 4, a piece-linear approximation of the iso-activity curves of copper, iron and nickel at 1273 K are presented. Those data were subsequently used for a piece-linear approximation of activities of Cu, Fe and Ni as a function of Cu and Fe concentration ($a_i(N_{Cu}, N_{Fe})$), where $i = \{Cu, Fe, Ni\}$ and applied for modelling of interdiffusion in Cu-Fe-Ni alloys.

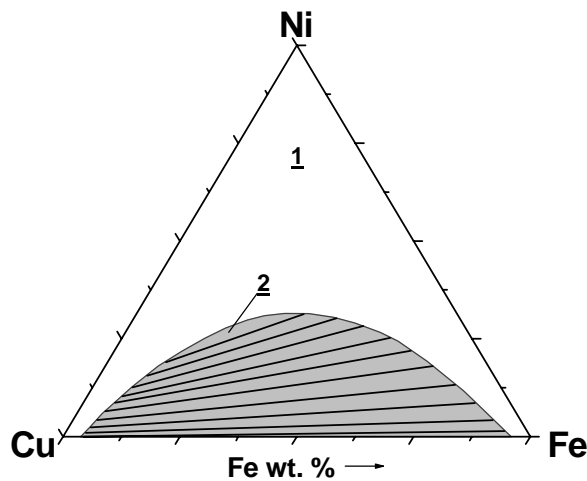


Figure 3. Ternary phase diagram Cu-Fe-Ni at 1273 K: 1 – single phase alloy, 2 – two phase alloy. The miscibility gap based on experimental results and thermodynamic reassessment [15].

Approximation of Radiotracer Diffusivities in Cu-Fe-Ni Alloys

The tracer diffusivities of Cu, Fe and Ni were obtained from radiotracer measurements for selected compositions of Cu-Fe-Ni alloys. However for the calculations we have to know functions, which describe the tracer diffusivities of Cu, Fe and Ni as a function of Cu and Fe concentration ($D_i^*(N_{Cu}, N_{Fe})$), where $i = \{Cu, Fe, Ni\}$). In the Figure 5 the Cu, Fe and Ni tracer diffusion coefficients are plotted as a function of the Cu and Fe concentration at 1271 K. Those diagrams were drawn using a polynomial approximation of the logarithm of Cu, Fe and Ni diffusivities, measured experimentally in the present work at selected compositions (Table 1).

Activity data (Fig. 4) and approximated tracer diffusion coefficients (Fig. 5) were applied to calculate the partial intrinsic diffusivities – Eq. (12), intrinsic fluxes – Eq. (11) and finally for modelling interdiffusion in the Cu-Fe-Ni Alloys.

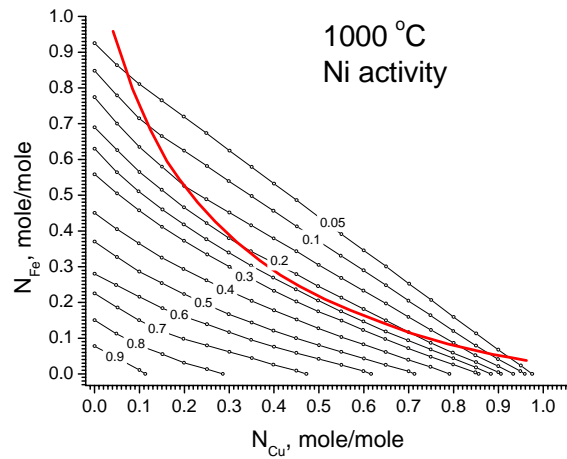
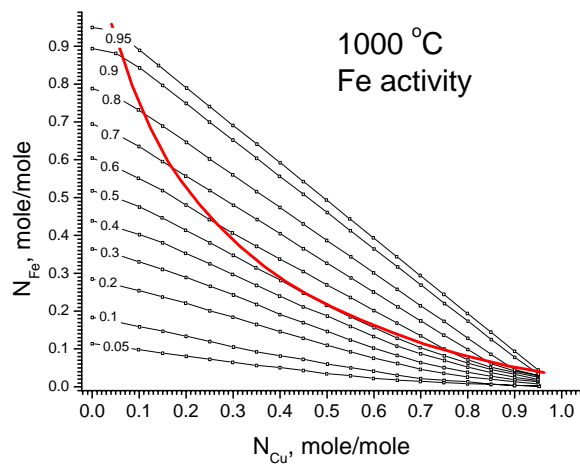
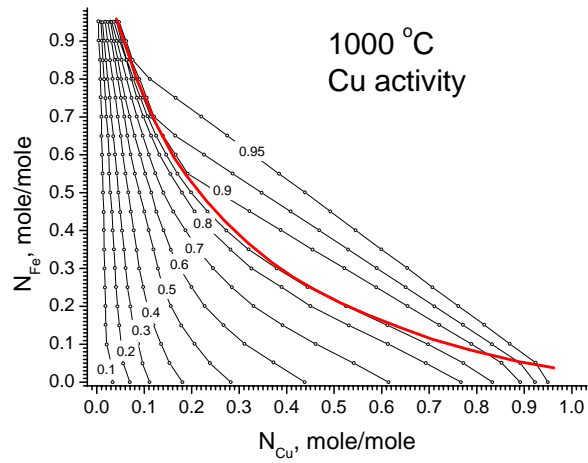


Figure 4. Iso-activity curves for Cu, Fe and Ni at 1273 K based on pure element reference state at 1273 K (1 atm) [15]. Bold solid line corresponds to the miscibility gap.

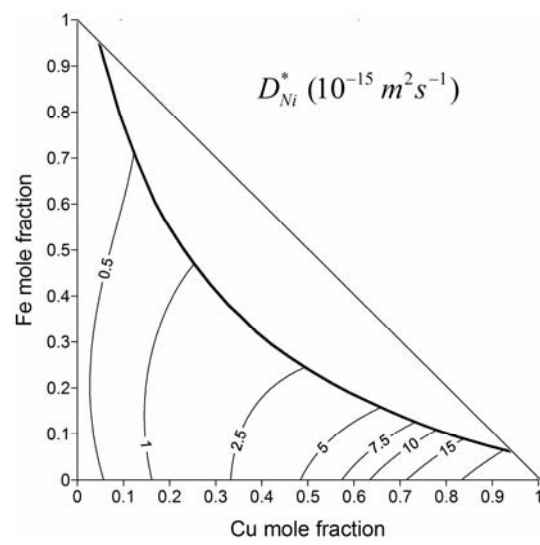
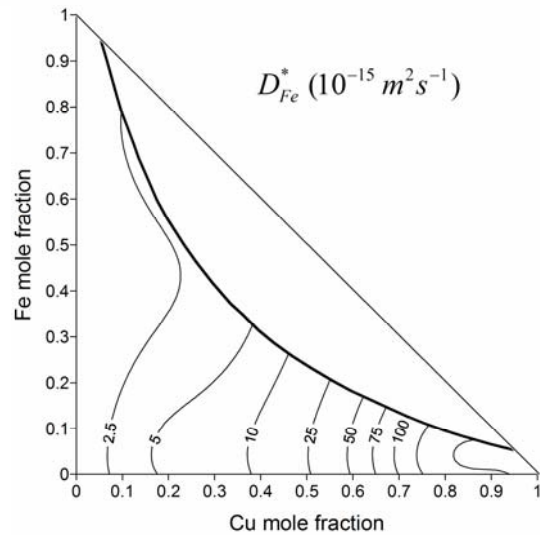
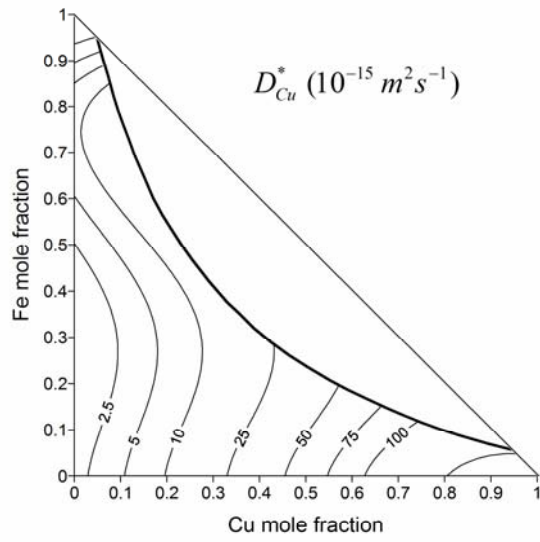


Figure 5. Cu, Fe and Ni tracer iso-diffusivity lines in Cu–Fe–Ni alloy at 1271 K. Bold solid line corresponds to the miscibility gap.

Modelling of Interdiffusion in the Cu-Fe-Ni Alloys

Interdiffusion modelling in the Cu-Fe-Ni alloys at 1273 K has been done using DIFSIM software [12]. Calculations have been done on a PC type computer. For the calculations the following data were used:

- (1) Initial concentration profiles – step functions defined by the terminal composition of the diffusion couples: Cu-48Ni | Fe-19.7Ni wt.% and Cu-58.1Ni | Fe-49.6 wt.% are shown in Figs. 6 and 7 respectively.
- (2) Average molar concentration of the Cu-Fe-Ni alloy, $c = 0.144 \text{ mol cm}^{-3}$.
- (3) Thickness of the diffusion couples, $2\Lambda = 0.07 \text{ cm}$.
- (4) Approximated tracer diffusion coefficients of copper, iron and nickel in Cu-Fe-Ni alloy – see Fig. 5.
- (5) Thermodynamic activity data – see Fig. 4.
- (6) Time of the process duration, $\hat{t} = 170 \text{ h}$.
- (7) Distance step in the calculations, 0.0014 cm .

The calculated concentration profiles of Cu, Fe and Ni were compared with the experimental results and show satisfactory agreement (Figs. 6 and 7).

Summary and Conclusions

Diffusion of ^{64}Cu , ^{59}Fe , and ^{63}Ni isotopes was measured in the Cu-Fe-Ni alloys of different compositions at 1271 K. Copper diffuses fastest while nickel is the slowest component in the system. It has been also found that when the Cu content in the alloys increases, the diffusivities also increase. Such behaviour correlates well with successive lowering of the melting temperature of corresponding alloys, as the Cu content increases.

The measured tracer diffusion coefficients of Cu, Fe, and Ni and the literature data on thermodynamic activities were used for modelling interdiffusion in the Cu-Fe-Ni diffusion couples. The calculated interdiffusion concentration profiles show satisfactory agreement with the experimental ones. This finding verifies the correctness of the Danielewski-Holly model and the assumptions made for the description of interdiffusion in non-ideal system.

Acknowledgments

This work was supported by the Polish State Committee for Scientific Research Grant No. 4T08A 001 25 during the period (2003-2005). Radiotracer production of the research reactor GKSS in Geesthacht, Germany is gratefully acknowledged.

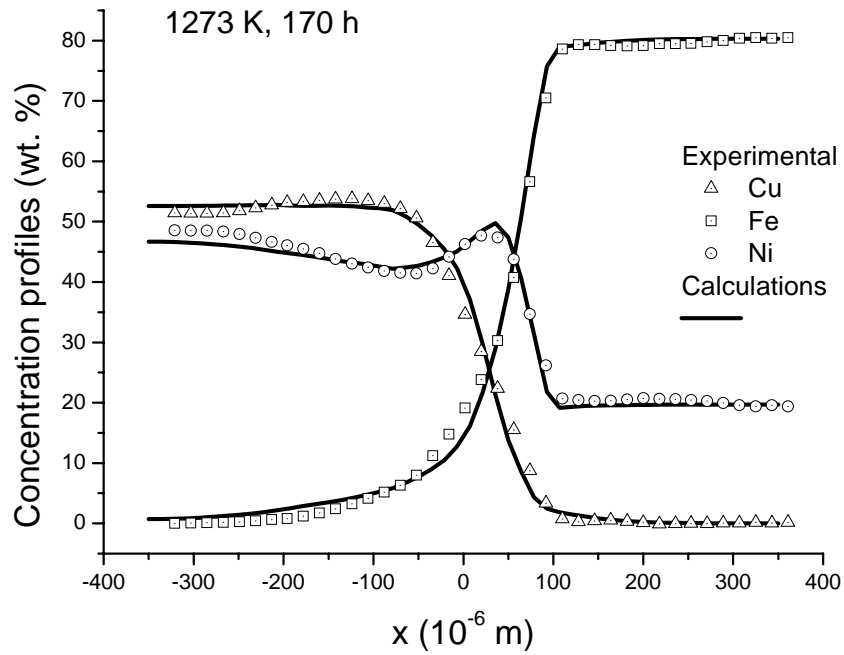


Figure 6. The calculated (solid lines) and experimental concentration profiles of the components in the Cu-48Ni/Fe-19.7Ni (wt.%) diffusion couple after 170 h of diffusion annealing at 1273 K in argon.

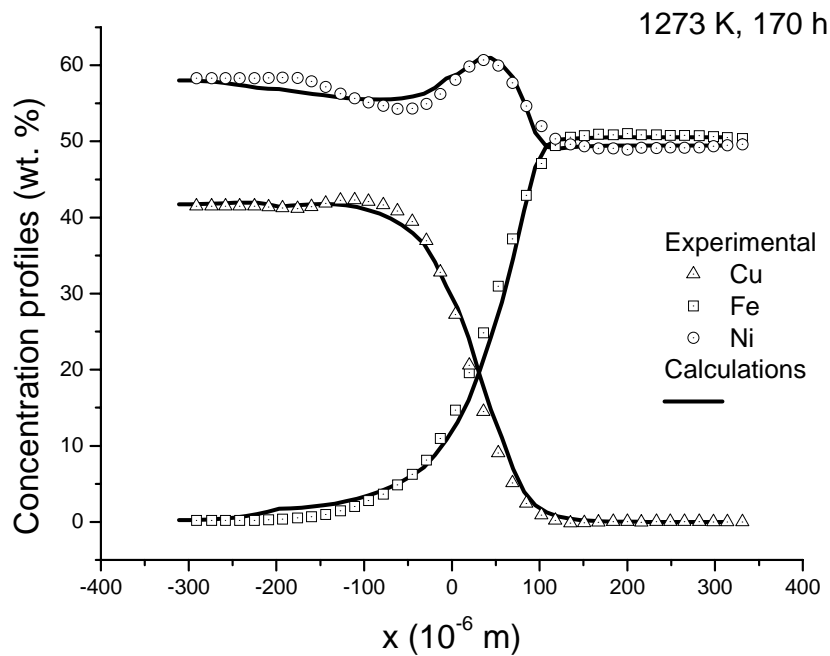


Figure 7. The calculated (solid lines) and experimental concentration profiles of the components in the Cu-58.1Ni/Fe-49.6 (wt.%) diffusion couple after 170 h of diffusion annealing at 1273 K in argon.

References

- [1] L. Onsager: Phys. Rev. Vol. 38 (1931), p. 2265
- [2] L.S. Darken: Trans. AIME Vol. 180 (1948), p. 430
- [3] C. Cserhati, Y. Ugaste, M.J.H. van Dal, N.J.H.G.M. Lousberg, A.A. Kodentsov and F.J.J. van Loo: Defect and Diffusion Forum Vol. 194-199 (2001), p. 189
- [4] K. Szyszkiewicz: *private communication*.
- [5] T. Suzuoka: J. Phys. Soc. Jpn. Vol. 19 (1964), p. 839
- [6] L.G. Harrison: Trans. Faraday Soc. Vol. 57 (1961), p. 1191
- [7] K. Holly and M. Danielewski: Phys. Rev. B Vol. 50 (1994), p.13336.
- [8] R. Filipek: Archives of Metallurgy and Materials Vol. 49 No. 2 (2004), p. 201
- [9] G. E. Murch: Diffusion Kinetics in Solids, Chapter in: Phase Transformations in Materials, G.Kostorz (Ed.), Wiley-VCH (2001), p.171.
- [10] M. Planck: Ann. Phys. Chem. (Wiedemann) Vol. 39 (1890), p. 161
- [11] A.C. Lasaga, *Kinetics in Earth Sciences*, Princeton University Press, 1998.
- [12] Demonstration version of the software is available at the web site
<http://ceram.agh.edu.pl/~rof/demo.html>
- [13] M. Danielewski and R. Filipek: J. Comp. Chem. Vol. 17 No. 13 (1996), p. 1497
- [14] A. Jansson: TRITA-MAC-0340 (The Royal Institute of Technology Stockholm 1987), p. 1
- [15] K. J. Rönkä, A. A. Kodentsov, P. J. J. Van Loon, J. K. Kivilahti and F. J. J. Van Loo: Metall. and Materials Transactions A Vol. 27A (1996), p. 2229.